

IMPROVE THE PERFORMANCE OF LTE USING OFDM/OQAM**1. Introduction**

In order to combat these impairments, many strategies have been invented. For example, turbo code as a channel coding method provides an effective solution to combat errors. Turbo codes are widely used in modern mobile communication systems, for instance, in the Long Term Evolution (LTE) and LTE-Advanced (LTE-A) standards [1]. To combat ISI, an approach called pre-coding can be employed. In the LTE and LTE-A standards, a pre-coding strategy named orthogonal frequency division multiplexing (OFDM) has been employed. The OFDM transmission can eliminate ISI almost completely [2], since in OFDM, the transmitted symbols are modulate into sub-carriers and each sub-carrier has narrow bandwidth, each symbol then observes a roughly frequency flat channel. However, one drawback of the OFDM is that it causes high peak-to-average power ratio (PAPR). As a consequence, more power will be consumed at the transmitter [3]. Power is a very limited and precious resource in a mobile communication system, especially for the up-link connection. Therefore, in the up-link channel of LTE and LTE-A system, another transmission scheme called single carrier frequency division multiple access (SC-FDMA) is employed. One important feature of SC-FDMA scheme is that it does not increase PAPR, thus it has better power efficiency [4,5]. Although SC-FDMA transmission scheme has low PAPR, it decreases the channel throughput when compared to OFDM transmission scheme, since it suffers from ISI. Recently, a novel equalization technology named multi-rate equalizer (MRE) has been proposed [6]. The MRE has low complexity implementation and increases the channel throughput at the same time [7]. Meanwhile, the MRE does not include any pre-coding. Thus, it does not increase PAPR and it can be implemented in SC-FDMA systems. In this thesis work, the MRE is implemented and simulated with time-invariant channel and Rayleigh fading channel models. Furthermore, we only consider binary phase shift keying (BPSK) with a fixed interweaver size. The performances are evaluated by examining how much throughput can be increased by employing the MRE. The simulation environment is built by using MATLAB software. LTE standard is established by 3rd Generation Partnership Project (3GPP) as the long term evolution of the Universal Mobile Telecommunications System (UMTS) networks. LTE standard was first proposed by NTT DoCoMo of Japan in 2004 and the studies of this new standard officially began in 2005. This standard is generally regarded as the next generation of mobile communications which can be used to implement 4G networks [8]. LTE standard is developed to achieve five main objectives. First one is to increase down-link and up-link peak data rates. Second one is to satisfy the demand for scalable bandwidth. The third one is to improve spectral efficiency continually. The fourth one is to design the network in all IP structure and the last one is to implement the standard based interface that can support a multitude of user types [8]. Due to these features, LTE mobile networks are capable of increasing the peak data rate to 100Mbps in the downlink channel and 86Mbps in the uplink channel. Furthermore, it can improve spectral efficiency to 5bps/Hz for the down-link and 2.5bps/Hz for the up-link. The cell edge performance (in terms of bit rate) is also improved with the reduction of connection latency [9]. There are three main technical characteristics in the LTE standard. First one is the OFDM transmission scheme is employed. This transmission scheme allocates transmitted sequence into sub-carriers. Each sub-carrier operates in a certain frequency which is orthogonal to others. OFDM enables high data bandwidth efficiency and providing a high tolerance to multi-path interference. In the up-link channel of LTE, SCFDMA is employed which can be considered as the discrete fourier transform (DFT) pre-coded OFDM [10]. The second characteristic is the utilization of multi-input and multi-output (MIMO) technique. The basic concept of MIMO is to use multiple transmit antennas and multiple receive antennas to increase the performance. The typical MIMO size includes

2×2 , 4×2 , 4×4 and 4×4 antenna configurations. It is easy to add further antennas in base station however in mobile station the number of antenna is limited, since the antennae are needed to be placed at least a half wavelength apart [11]. The third one is the implementation of system architecture evolution (SAE). In SAE, one improvement is that a number of functions which is previously executed in the core network have been transferred out to periphery. Therefore, it can provide a much flatter form of network architecture and as a consequence, the latency time can be reduced [12,13]. Despite SC-FDMA transmission has lower PAPR, it has a performance loss when compared it to OFDM transmission. In OFDM transmission, each sub-carrier has a narrow bandwidth and it is modulated by different symbol. Thus, in the frequency selective channel, each symbol observes a roughly frequency flat channel. However, in SC-FDMA transmission, a group of sub-carriers are modulated by the same symbol. Therefore, the bandwidth of each symbol has a relatively wider bandwidth and it cannot be assumed as frequency flat. This frequency selectivity causes ISI. As a consequence, in SC-FDMA transmission, an equalizer is needed to combat the ISI [13, 14].

2. Analysis of published data and problem statement

Orthogonal frequency division multiplexing (OFDM) attracts a lot of attention for high speed wireless transmissions because of its capability to cope with frequency selective radio links, turning the wideband channel into several narrow-band subchannels, whose equalization can be independently performed in a simple way.

The OFDM solution that employs a prototype filter with square impulse response. In such a case no polyphaser filtering is needed and intersymbol and intercarrier interference (ISI and ICI) can be easily avoided adding a suitable cyclic extension before data transmission. To our knowledge, the issue of OFDM-OQAM transmissions over noisy frequency selective channels has received less attention in literature. In [7] authors have compared, by means of simulations, OFDM-OQAM with the DMT solution pointing out the better bit error rate achievable by OFDM-OQAM.

3. Purpose and objectives of the study

This solution, referred to as DMT (discrete multitone) with cyclic prefix, in spite of its simple structure and robustness to frequency selective channels presents some drawbacks, such as spectral efficiency loss due to the cyclic prefix insertion, high sensitivity to residual frequency offsets, phase noise, and fast time variations of the channel.

These weaknesses have roused researchers' interest for other OFDM architectures. In particular, herein, it is considered the scheme proposed in [2] named OFDM-OQAM. The main idea lies in transmitting Offset quadrature amplitude modulation symbols (also called staggered QAM), instead of conventional Quadrature Amplitude Modulation ones, on each OFDM subcarrier. In order to retain orthogonality among subchannels the shape of the prototype filter should be chosen in order to comply with the reconstruction conditions [2-7]. For this reason, most of the publications concerning with OFDM-OQAM have dealt with the design of filters capable of ISI and ICI free transmissions, e.g., [3], [4]. The efficient implementation of OFDM-OQAM architecture has been addressed in [5] and [6], where the modulation scheme has been studied in the mirror assuming transmissions over memoryless noiseless channels.

That gain was explained observing that, since OFDM-OQAM does not require the cyclic prefix, for the same spectral efficiency the code rate can be increased taking better advantage of the coding gain and frequency selectivity introduced by the channel. The promising results of [7] have been emphasized by the 3GPP standardization forum which has recently considered OFDM/OQAM suitable for improved downlink UTRAN interfaces [8].

4. Base principle of OFDM/OQAM

Offset in OQAM express the time shift of half the inverse of the sub-channel spacing between the real and imaginary parts of a complex symbol. The data will be sent on the real and the imagi-

nary part of samples alternatively. In OQAM, The throughput rate will stay as in Quadrature Amplitude Modulation as used in orthogonal frequency division multiplexing systems, but without inserting the guard time [4]. To represent OQAM signals we can start from a Quadrature Amplitude Modulation signal constellation.

First let us assume the QAM symbol is as a complex quantity, and then $C_{m,l}$ can be expressed in the formula:

$$C_{m,l} = C_{m,l}^R + jC_{m,l}^I, \quad (1)$$

where carries the information to be transmitted over sub-channel during the frame of bits. And is the real part is the imaginary part of.

The principle of OFDM/OQAM is illustrated in Figure 1. The subcarriers are evenly spaced, $\Delta f = 1/T$, where T is the symbol period. The system can resist ISI and ICI by taking the merit of the orthogonality between subcarriers and the perfect reconstruction (PR) condition of the prototype filter [15]. At the transmitter the complex symbols are:

$$x_k(n) = s_k^I(n) + js_k^O(n), \quad (2)$$

where $s_k^I(n)$ and $s_k^O(n)$ are the real and imaginary parts of the n th symbol in the k^{th} subcarrier. Then, the quadrature component is delayed by half of a symbol period $T/2$ with respect to the in-phase component, which forms the modulation of offset QAM

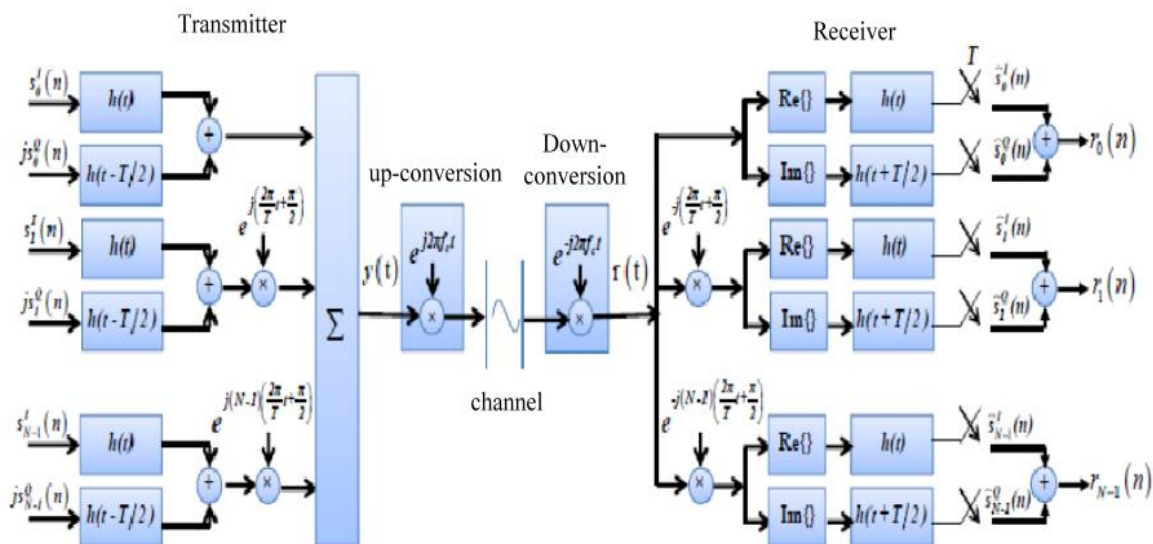


Fig. 1. Principle of OFDM/OQAM

Both of the in-phase and quadrature components are then fed into the designed filters $h(t)$ and modulated onto N subcarriers, which is written as:

$$y(t) = \sum_{k=0}^{N-1} \sum_{n=0}^{+\infty} \left[s_k^I(n) \cdot h(t-nT) + js_k^O(n) \cdot h(t-nT - \frac{T}{2}) \right] e^{jk\varphi_t}, \quad (3)$$

where $h(t)$ is the impulse response of the prototype filter, and $\varphi_t = \frac{2\pi f_c t}{T} + \frac{\pi}{2}$. When the OFDM/OQAM baseband is formed, it is then up-converted to a wireless or optical channel. At the receiver, the analog signal $r(t)$ is demodulated and then fed into the corresponding matched filters. The filtered signal is then sampled at rate of $1/T$. The output symbol on k th subcarrier is given as:

$$r_k(n) = \widehat{s}_k^I(n) + j\widehat{s}_k^Q(n) , \quad (4)$$

where $\widehat{s}_k^I(n)$ and $\widehat{s}_k^Q(n)$ are the real and imaginary parts of the n th received symbol on the k th sub-carrier, respectively. From [16]:

$$\Re\left\{\langle g_{m,n} | g_{p,q} \rangle\right\} = \Re\left\{\int g_{m,n}(t)g_{p,q}(t)dt\right\} = \delta_{m,p}\delta_{n,q} \quad (5)$$

and

$$\widehat{s}_k^I(n) = \sum_{n'=-\infty}^{+\infty} \sum_{k'=0}^{N-1} \int_{-\infty}^{+\infty} h(nT-t+\frac{T}{2})x\left\{s_{k'}^I(n)h(t-n'T)\sin[(k'-k)\varphi_i] - s_{k'}^Q(n)h(t-n'T-\frac{T}{2})\cos[(k'-k)\varphi_i]\right\}dt . \quad (6)$$

If the filter response $h(t)$ is real and even (i.e., $h(t) = h(-t)$), and meets the PR condition, which is given in the following equations, then the received signal can be recovered:

$$\int_{-\infty}^{+\infty} h(t-n'T)h(nT-t)\cos[(k'-k)\varphi_i]dt = \delta(k'-k, n'-n) , \quad (7)$$

$$\int_{-\infty}^{+\infty} h(t-n'T/2)h(nT-t)\sin[(k'-k)\varphi_i]dt = 0 , \quad (8)$$

$$\int_{-\infty}^{+\infty} h(t-n'T)h(nT-t+T/2)\sin[(k'-k)\varphi_i]dt = 0 , \quad (9)$$

$$\int_{-\infty}^{+\infty} h(t-n'T/2)h(nT-t+T/2)\cos[(k'-k)\varphi_i]dt = \delta(k'-k, n'-n) . \quad (10)$$

The prototype filter $h(t)$ is designed to not only contribute great stop band attenuation, but also compensate the optical channel dispersion [17]. Note that, the direct implementation of OFDM/OQAM system depicted in Fig.1 would be very costly. However, it can be realized by an efficient FFT/IFFT-based implementation [18], which has also been used in our demonstrations. Without loss of generality, we assume that $h(t)$ is a square-root raised cosine filter (roll off factor in the simulation for Fig. 2 is 0.5). The rectangular time response used in conventional orthogonal frequency division multiplexing is also shown in Figure 2 for comparison. The frequency domain response clearly shows that the side bands of OFDM/OQAM are significantly suppressed.

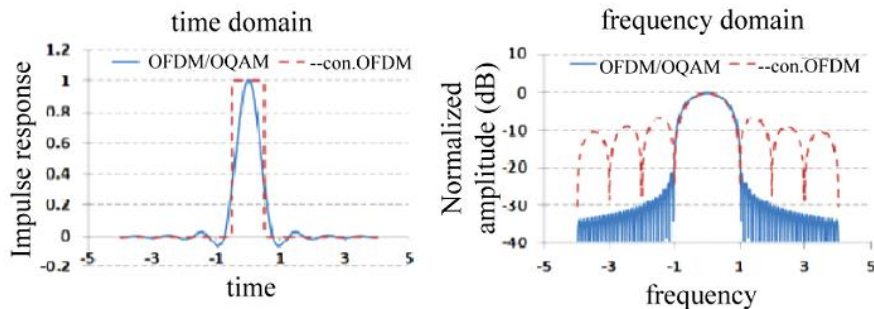


Fig. 2. Time and frequency domain impulse response

Figure 3 shows two spectra of conventional OFDM and OFDM/OQAM. As shown in the Figure 3, the side lobe suppression ratio of OFDM/OQAM system is much higher (>35dB) than the conventional Orthogonal frequency division multiplexing (~15 dB).

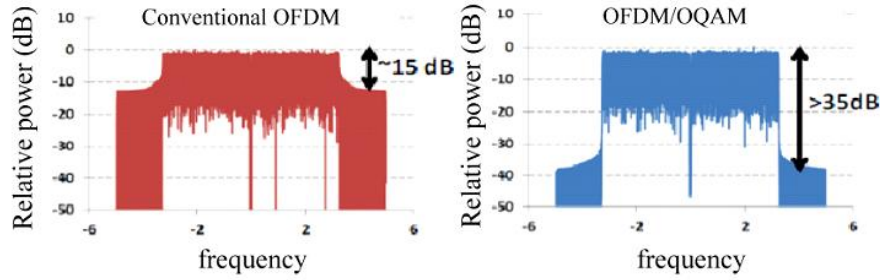


Fig 3. Frequency spectra for conventional OFDM and OFDM/OQAM

5. OFDM/OQAM mathematical model

The previous section demonstrated the principles of the OQAM and the continuous time model of the system. This section focuses on the presentation of the discrete time mathematical model and the orthogonality condition of the OQAM. The staggering of the complex Quadrature Amplitude Modulation coefficients can be pre-processed prior to the modulation process. Thus, the discrete time OQAM signal can be written as [19, 20]:

$$s[k] = \sum_{m=0}^{M-1} \sum_{n=-\infty}^{\infty} a_{m,n} g[k - nN] e^{j \frac{2\pi m}{M} (k - \frac{L-1}{2})} e^{j\phi_{m,n}}, \quad (11)$$

with

$$\phi_{m,n} = \phi_0 + \frac{\pi}{2} (m + n),$$

where $N=M/2$ represents discrete time offset with M has to be even number, while $\phi_{m,n}$ is an additional phase term in which ϕ_0 can be arbitrarily chosen. The real-valued coefficient $a_{m,n}$, holds either real or imaginary part of the staggered complex Quadrature Amplitude Modulation coefficient. L indicates the length of the prototype filter g , that can take an integer multiple of M such as: $L=km$; is called overlapping factor with $K>0, K \in \mathbb{Z}$.

Assuming that the prototype filters of the OQAM have unity energy (normalised), the subcarrier filters are attained by uniformly frequency shifting single low-pass FIR prototype filter. Consequently, the synthesis filter bank, as depicted in Figure 4 can be expressed as [19, 20]:

$$Tx_m[k] = g[k] e^{j \frac{2\pi m}{M} (k - \frac{L-1-N}{2})}, \quad (12)$$

while the analysis filterbank can be written as:

$$Rx_m[k] = g[k] e^{j \frac{2\pi m}{M} (k - \frac{L-1-N}{2})} = Tx_m^*[L-1-k], \quad (13)$$

for all $m=0, 1, \dots, M-1$ and $k=0, 1, \dots, L-1$. If the prototype filter g is assumed to be real and symmetrical, as in the rest of this thesis, then $Rx_m[k]=Tx_m[k]$ for all m and k .

The Gabor function in this case is the term $g_{m,n}[k]$ in (2.49) from which the orthogonality condition can be calculated such as:

$$\text{Re} \langle g_{m,n}, g_{p,q} \rangle = \text{Re} \left\{ \sum_{k=0}^{L-1} g_{m,n}[k] g_{p,q}^*[k] \right\} = \delta_{m,p} \delta_{n,q}, \quad (14)$$

where $\delta_{m,p}$ and $\delta_{n,p}$ are both Kronecker deltas. If $m,n \neq p,q$, then the inner product $\langle g_{m,n}, g_{p,q} \rangle$ is a pure imaginary term.

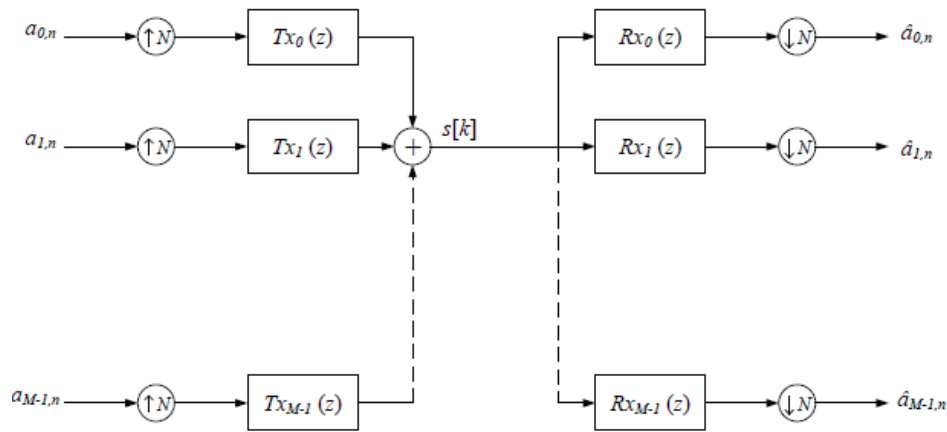


Fig.4. Structure of OFDM/OQAM system in discrete time

In theory, the prototype filter g can be designed to produce TMUX configuration that can accomplish perfect reconstruction (PR) of the transmitted data at the receiver side. By assuming a distortion free channel and an ideal transmission process, then the received signal with these PR filters is just delayed version of the transmitted signal. On the other hand, the prototype filter can be designed to produce nearly perfect reconstruction (NPR). As a result, some marginal levels of ISI and ICI are present even in the case of distortion free channel. However, during the design process of the filter, the level of interference can be kept to minimum. These NPR filters offer more freedom in the filter design process to achieve higher level of stop-band attenuation than the PR with the same length [20-21]

6. The OFDM/OQAM modulation

Possible write the baseband equivalent of a continuous-time OFDM/OQAM signal as follows [1]:

$$s(t) = \sum_{m=0}^{M-1} \sum_{n \in \mathbb{Z}} a_{m,n} g(t - n\tau_0) e^{j2\pi m F_0 t} e^{j\phi_{m,n}} \quad (13)$$

They are obtained from a $2K$ -QAM constellation, taking the real and imaginary parts of these complex-valued symbols of duration $T_0 = j2\pi$, where ζ_0 denotes the time offset between the two parts [1, 3, 8]. Assuming a distortion-free channel, perfect reconstruction of real symbols is obtained owing to the following real orthogonality condition:

$$\Re \left\{ \langle g_{m,n} | g_{p,q} \rangle \right\} = \Re \left\{ \int g_{m,n}(t) g_{p,q}(t) dt \right\} = \delta_{m,p} \delta_{n,q} \quad (14)$$

where, $\pm m; p = 1$ if $m = p$ and $\pm m; p = 0$ if $m \neq p$.

For concision purpose is set $hgip; q m; n = ij hgm; njgp; qi$, with $hgm; njgp; qi$ a pure imaginary term for $(m; n) \neq (p; q)$. However in practice for transmission over a realistic channel, the orthogonality property is lost, leading to Inter Symbol Interference and ICI (Inter Carrier Interference). We will show that if the prototype filter g has good localization properties in time and frequency domains, a simple one tap equalization process may be sufficient to restore the real orthogonality. However, this equalization requires channel estimates that are complex-valued. As the orthogonality is limited to the real field a specific estimation procedure has to be carried out. Recall that in practical orthogonal frequency division multiplexing systems the complex orthogonality is insured thanks to the introduction of a cyclic prefix (CP) of length ζ .

8. Conclusion

This solution, referred to as DMT (discrete multitone) with cyclic prefix, in spite of its simple structure and robustness to frequency selective channels presents some drawbacks, such as spectral efficiency loss due to the cyclic prefix insertion, high sensitivity to residual frequency offsets, phase noise, and fast time variations of the channel. These weaknesses have roused researchers' interest for other OFDM architectures. In particular, herein, it is considered the scheme proposed in named OFDM-OQAM. The main idea lies in transmitting Offset quadrature amplitude modulation symbols, instead of conventional Quadrature Amplitude Modulation ones, on each OFDM subcarrier. In order to retain orthogonality among subchannels the shape of the prototype filter should be chosen in order to comply with the reconstruction conditions.

References: 1. Holma H., & Toskala A. (2011) LTE for UMTS: Evolution to LTE-Advanced. Wiley Press, New York. 2. Cho Y.S., Jeon W.G., & Chang K.H. (1999) An Equalization Technique for Orthogonal Frequency-division Multiplexing Systems in Time-variant Multipath Channels. IEEE Transactions on Communications (Volume:47, Issue: 1), pp.27-32. 3. Priyanto B.E., Codina H., Rene S., Sorensen T.B., Mogensen P. (2007) Initial Performance Evaluation of DFT-Spread OFDM Based SC-FDMA for UTRA LTE Uplink. IEEE Vehicular Technology Conference, Dublin, pp. 3175-3179. 4. Borko F., & Syed A.A. (2009) Long Term Evolution: 3GPP LTE Radio And Cellular Technology. Auerbach Publications, Boca Raton USA. 5. Moray R. (2009) LTE and the Evolution to 4G Wireless: Design and Measurement Challenges. John Wiley and Sons Press, New York. 6. Fatih M.B., & Juntti M. (2013) A Multirate Equalizer for Inter-Symbol Interference Channels Based on Successive Interference Cancellation. Proceeding Personal Indoor and Mobile Radio Communications (PIMRC), 2013 IEEE 24th International Symposium on. London, United Kingdom, pp. 702-706. 7. Goodman D.J., Myung H.G., & Lim J. (2006) Peak-to-Average Power Ratio of Single Carrier FDMA Signals with Pulse Shaping. Proceeding of The 17th Annual IEEE International Symposium on Personal, Indoor and Mobile Radio Communications, Helsinki, Finland, pp. 1-5. 8. Christoph C. (2012) An Introduction to LTE: LTE, LTE-Advanced, SAE and 4G Mobile Communications. John Wiley and Sons Press, New York. 9. (2009) LTE An End-to-End Description of Network Architecture and Elements. 3GPP LTE Encyclopedia. 10. Robertson P., & Kaiser S. (1999) The effects of Doppler spreads in OFDM(A) mobile radio systems. Vehicular Technology Conference, 1999. VTC 1999 - Fall. IEEE VTS 50th (Volume:1), pp. 329 - 333. 11. Bahai A., Cui S., & Goldsmith A.J. (2004) Energy-efficiency of MIMO and Cooperative MIMO in Sensor Networks. Selected Areas in Communications // IEEE Journal on (Volume:22, Issue:6), pp. 1089-1098. 12. (2007) 3GPP TS 23.002: Network Architecture. 3GPP SP- 63 Release-12, Fukuoka, Japan. 13. Goodman D., Myung H.G., & Junsung L. (2006) Single Carrier FDMA for Uplink Wireless Transmission. IEEE Vehicular Technology Magazine vol. 1, no. 3, pp. 30-38. 14. Falconer D., Falconer D., Ariyavitakul S.L., Benyamin-Seeyar A., & Eidson B. (2002) Frequency Domain Equalization for Single-Carrier Broadband Wireless Systems. IEEE Commun. Mag., vol.40, no.4, pp. 58-56. 15. P. Amini, R. Kemper and B. Farhang-Boroujeny. A comparison of alternative filterbank multicarrier methods in cognitive radio systems // Proceedings of SDRTC' 2006. 16. D. Chen, D. Qu and T. Jiang Novel prototype filter design for FBMC based cognitive radio systems through direct optimization of filter coefficients // Proceedings of WCSP'2010. 17. K. Arya and C. Vijaykumar. Elimination of Cyclic Prefix of OFDM systems using filter bank based multicarrier systems // TENCON IEEE Region 10 Conference. IEEE, 2008. 18. L. Vangelista and N. Laurenti. Efficient implementations and alternative architectures for OFDM-OQAM systems // IEEE Trans. Commun. 49(4), 664-675 (2001). 19. P. Siohan, C. Siclet, and N. Lacaille. Analysis and design of OFDM/OQAM systems based on filterbank theory // Signal Processing, IEEE Transactions on, vol. 50, pp. 1170-1183, 2002. 20. T. Ihalainen, A. Viholainen, T. H. Stitz, and M. Renfors. Generation of Filter Bank-Based Multicarrier Waveform Using Partial Synthesis and Time Domain Interpolation // Circuits and Systems I: Regular Papers, IEEE Transactions on, vol. 57, pp. 1767-1778, 2010. 21. P. P. Vaidyanathan. Multirate Systems and Filter Banks. Englewood Cliffs, NJ: Prentice Hall Inc., 1993.

Харьковский национальный
университет радиоэлектроники

Поступила в редколлегию 14. 02. 2016